Article

pubs.acs.org/Biomac

Peptide Anchor for Folate-Targeted Liposomal Delivery

Eugénia Nogueira,[†,‡] Irene C. Mangialavori,[§] Ana Loureiro,[†,‡] Nuno G. Azoia,[‡] Marisa P. Sárria,[‡] Patrícia Nogueira,[∥,⊥] Jaime Freitas,[∥,⊥] Johan Härmark,[#] Ulyana Shimanovich,[▽] Alexandra Rollett,[○] Ghislaine Lacroix,[◆] Gonçalo J. L. Bernardes,[▽] Georg Guebitz,[○] Hans Hebert,[#] Alexandra Moreira,[∥,⊥] Alexandre M. Carmo,[∥,⊥,¶] Juan Pablo F. C. Rossi,[§] Andreia C. Gomes,[†] Ana Preto,[†] and Artur Cavaco-Paulo*[,‡]

[†]CBMA − Centre of Molecular and Environmental Biology, Department of Biology, University of Minho, Braga 4710-057, Portugal

[‡]CEB − Centre of Biological Engineering, University of Minho, Braga 4710-057, Portugal

[§]IQUIFIB − Instituto de Química y Fisicoquímica Biológicas, Facultad de Farmacia y Bioquímica, Universidad de Buenos Aires, CONICET, 1113 Buenos Aires, Argentina

[∥]Instituto de Investigação e Inovação em Saúde, Universidade do Porto, Porto, Portugal

[⊥]IBMC − Instituto de Biologia Molecular e Celular, 4150-180 Porto, Portugal

[#]Department of Biosciences and Nutrition, The Royal Institute of Technology, School of Technology and Health, Karolinska Institutet, S-14183 Huddinge, Sweden

[▽]Department of Chemistry, University of Cambridge, Cambridge CB2 1EW, United Kingdom

[○]Institute of Environmental Biotechnology, University of Natural Resources and Life Sciences, 3430 Tulln, Austria

[◆]INERIS - Institut National de l'Environnement Industriel et des Risques, 60550 Verneuil en Halatte, France

[¶]ICBAS − Instituto de Ciências Biomédicas Abel Salazar, Universidade do Porto, 4099-003 Porto, Portugal

Supporting Information

ABSTRACT: Specific folate receptors are abundantly overexpressed in chronically activated macrophages and in most cancer cells. Directed folate receptor targeting using liposomes is usually achieved using folate linked to a phospholipid or cholesterol anchor. This link is formed using a large spacer like polyethylene glycol. Here, we report an innovative strategy for targeted liposome delivery that uses a hydrophobic fragment of surfactant protein D linked to folate. Our proposed spacer is a small 4 amino acid residue linker. The peptide conjugate inserts deeply into the lipid bilayer without affecting liposomal integrity, with high stability and specificity. To compare the drug delivery potential of both liposomal targeting systems, we encapsulated the nuclear dye Hoechst 34580. The eventual increase in blue fluorescence would only be detectable upon liposome disruption, leading to specific binding of this dye to DNA. Our delivery system was proven to be more efficient (2-fold) in Caco-2 cells than classic systems where the folate moiety is linked to liposomes by polyethylene glycol.

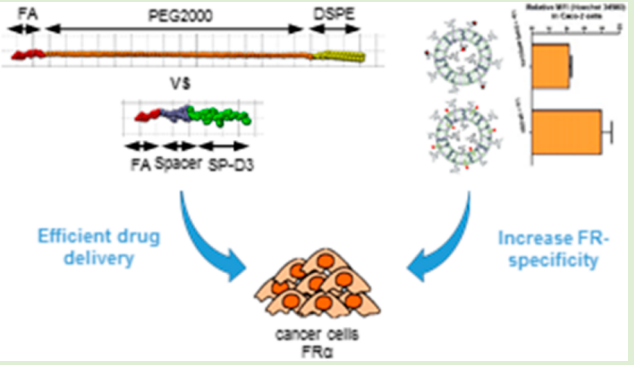

INTRODUCTION

Liposomes have gained extensive attention as carriers for a wide range of drugs due to properties such as sustained release, altered pharmacokinetics, increased drug stability, ability to overcome drug resistance, and target specific tissues.[1] Folate receptor (FR), one of the most studied molecular targets for directed therapy, is a glycoprotein with high affinity for folate (or folic acid, FA) ($K_d \sim 100$ pM).[2,3] Two main membrane variants of the FR exist, FRα and FRβ. FRα is overexpressed in about 40% of human carcinomas. FRβ, by contrast, is expressed in its functional form on activated macrophages and myelogenous leukemia blasts.[4] Both these FRs are absent in most normal tissues. FR-targeting liposomes, with FA covalently attached via a polyethylene glycol (PEG) linker to a phospholipid or cholesterol (CH) anchor and incorporated into the bilayer during liposome preparation, were previously developed.[5−8] Although these FA conjugates were shown to successfully target FR-overexpressing cancer cells, self-aggregation of FA at the liposome surface has often been observed when using such formulations, leading to reduced FR targeting

Received: June 19, 2015
Revised: July 29, 2015

DOI: 10.1021/acs.biomac.5b00823
Biomacromolecules XXXX, XXX, XXX−XXX

efficiency.[6] Furthermore, there are concerns over the two negative charges carried by FA-PEG-phospholipid and the use of a carbamate linker in FA-PEG-CH, which has limited hydrolytic stability.[9]

Here, we report the design of a bifunctional peptide, derived from the neck domain of pulmonary surfactant-associated protein D (SP-D),[10] that simultaneously serves as an FA linker and as an anchor. Mammalian pulmonary surfactant proteins can, in nature, promote the self-assembly of phospholipids toward zero potential interface,[11] suggesting that fragments or models of these proteins are capable of recognizing and interacting with liposomal phospholipids. These findings prompted us to investigate the use of pulmonary surfactant proteins for the preparation of targeted liposomes. The α-helical neck region of SP-D shows an affinity for phospholipids and thus might promote the binding of SP-D to these structures,[12] further supporting their potential use as linker and anchor for FA conjugates. We designed several subsets of liposome formulations to show the funtionality of our final system containing the peptide SP-DS3. Their lipid membrane insertion ability was extensively characterized, and tests were performed to evaluate the potential of this formulation as a specific drug delivery system.

EXPERIMENTAL SECTION

Materials. 1,2-Dioleoyl-*sn*-glycero-3-phosphoethanolamine (DOPE) and *N*-(carbonyl methoxypolyethylene glycol-2000)-1,2-distearoyl-*sn*-glycero-3-phosphoethanolamine (DSPE-MPEG) were obtained from Lipoid GmbH (Germany), and DSPE-PEG-FA was obtained from Avanti Polar Lipids (USA). CH, fluorescein isothiocyanate (FITC), carbon monoxide-releasing molecule-2 (CORM-2) and methotrexate (MTX) were obtained from Sigma (USA). Celecoxib was obtained from Cadila Pharmaceuticals, Ltd. (India).

Peptide Synthesis. The neck-domain peptides constructed from SP-D were synthesized by JPT Peptide Technologies GmbH (Berlin, Germany) and American Peptide (Sunnyvale, CA, USA). FA was covalently bound at the N-terminus of the peptides via glutamic acid and pteroic acid, using a standard Fmoc-based solid-phase synthesis protocol. Benzotriazole-1-yl-oxy-tris-pyrrolidino phosphoniumhexafluorophosphate was applied as the activating reagent to ensure efficient coupling. Fmoc protecting groups were removed after every coupling step under standard conditions (20% piperidine in DMF). Oregon Green 488 was covalently bound at the C-terminus. Peptides were purified to greater than 75% homogeneity, as determined by analytical high-performance liquid chromatography (Supporting Information Figure S1), and characterized by mass spectrometry (Figure S2).

Liposome Preparation. Liposomes composed of DOPE/CH/DSPE-MPEG were prepared using a thin film hydration method. Briefly, known amounts of DOPE, CH and DSPE-MPEG were dissolved in chloroform in a 50 mL round-bottom flask. In liposomes with DSPE-PEG-FA, this compound was also added in this step. For macrophage internalization studies, FITC was incorporated in the lipidic film, in the hydrocarbon region of the bilayer. The organic solvent was evaporated using a rotary evaporator followed by additional evaporation under reduced pressure by a high-vacuum system to remove remaining traces of chloroform. The resultant dried lipid film was dispersed in phosphate-buffered saline (PBS) buffer containing either peptides. The mixture was vortex-mixed at a temperature greater than the phase-transition temperature (room temperature) to yield multilamellar vesicles, which were then extruded (extruder supplied by Lipex Biomembranes Inc., Vancouver, Canada) through 200 nm pore size polycarbonate filters (Nucleopore) followed by several passages through 100 nm polycarbonate filters (Nucleopore) to form large unilamellar vesicles. The free peptide and drugs that were not incorporated into liposomes were removed from the samples after passage through a gel filtration chromatography column (GE Healthcare), with 5 kDa cutoff (PD-10 Desalting Columns containing 8.3 mL of Sephadex G-25 Medium).

Determination of the Zeta Potential and Size Distribution. The zeta-potential (ζ-potential) values and size distribution of liposomes were determined at pH 7.4 (PBS buffer) and 25.0 °C by electrophoretic laser Doppler anemometry and photon correlation spectroscopy (PCS), respectively, using a Malvern Zetasizer NS (Malvern Instruments). The lipid concentration was held constant at 400 μM. The viscosity and refractive index values were 0.890 cP and 1.330, respectively.

Folic Acid Quantification. The quantification of FA present at the liposomal surface was performed using a RIDASCREEN FAST Folic Acid kit (R-Biopharm, Germany) according to the manufacturer's instructions. This kit is a competitive enzyme immunoassay and quantifies the folic acid at the liposomal surface.

Fluorescence Spectroscopy. Fluorescence experiments were performed using a Fluorolog spectrofluorometer (JY Horiba) with a 1 × 1 cm quartz cell thermostated at 25.0 °C. The band-pass of the excitation slit was set to 2.0 nm to obtain an optimal signal-to-noise ratio without photodegradation. Fluorescence was excited at 280 nm, and the emission was scanned from 310 to 450 nm at an increment of 1 nm and an integration time of 1 s.

Hydrophobic Photolabeling. The photoactivatable phosphatidylcholine analogue [^{125}I]TID-PC/16 was prepared as described by Mangialavori et al. (2009).[13] A dried film of the photoactivatable reagent [^{125}I]TID-PC/16 was suspended in 0.005% C12E10 and liposomes incorporating SP-DS3. The samples were incubated for 20 min at room temperature in the dark before being irradiated for 20 min with light from a filtered UV source (λ = 366 nm).

Radioactivity and Protein Determination. Electrophoresis was performed according to the Tris-Tricine SDS-PAGE method. Peptide was stained with Coomassie BlueR, the isolated bands were excised from the gel, and the incorporation of radioactivity was directly measured with a gamma counter. The amount of protein was quantified by eluting each stained band, including bovine serum albumin, in each gel for protein quantification. Specific incorporation was calculated as the ratio between the measured radioactivity and the amount of protein determined for each band.

Molecular Dynamics Simulations. The simulations were performed with the GROMACS 4.0.7[14] package using the Gromos ffG43a1 force field. The bond lengths were constrained using LINCS.[15] Nonbonded interactions were calculated using a twin-range method with short- and long-range cut-offs of 0.8 and 1.2 nm, respectively. Neighbor searching was updated every five steps. An integration time step of 2 fs was used. A reaction field correction for the electrostatic interactions was applied using a dielectric constant of 15. Pressure control was implemented using a Berendsen barostat[16] with a reference pressure of 1 bar, a relaxation time of 0.5 ps and an isothermal compressibility of 4.5×10^{-5} bar^{-1}. Temperature control was set at 300 K using a Berendsen thermostat.[16] Each component of the system was included in separate heat baths with temperature coupling constants of 0.1 ps. Five replicate simulations were performed using different initial velocities determined from a Maxwell–Boltzmann distribution at 300 K.

Electron Microscopy Imaging. For scanning transmission electron microscopy (STEM) analysis, a liposomal suspension was dropped onto carbon film over copper grids (400 mesh, 3 mm diameter). The shape and morphology of the liposomes were observed using a NOVA Nano SEM 200 FEI system. For transmission electron microscopy (TEM) analysis, the liposome samples were diluted 1:20 in distilled water and applied to glow-discharged carbon-coated copper grids followed by negative staining with a solution of 1% (w/v) uranyl acetate. Imaging was performed using a JEOL JEM2100F transmission electron microscope operating at an acceleration voltage of 200 kV. Images were recorded with a 4k*4k CCD camera (Tietz Video and Image Processing Systems GmbH, Gauting, Germany) at a magnification of 100 000×.

Cell Culture Conditions. The human colonic epithelial cell line (Caco-2) (ATCC, HTB-37) was obtained from the American Type

DOI: 10.1021/acs.biomac.5b00823
Biomacromolecules XXXX, XXX, XXX−XXX

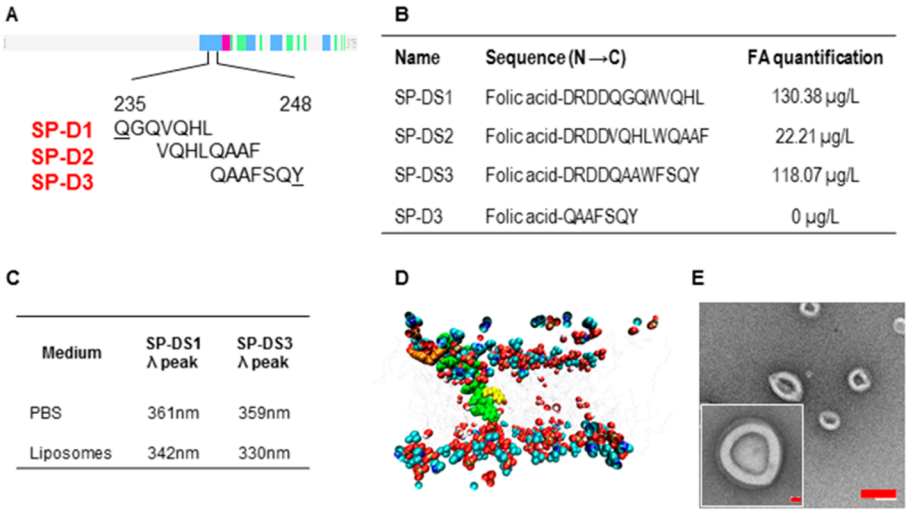

Figure 1. SP-DS3 peptide, derived from pulmonary surfactant-associated protein D, is deeply inserted into the liposomal bilayer with FA at the liposomal surface. (A) Diagram of the analyzed SP-D fragments. The localization in the SP-D sequence is indicated, and numbers correspond to the amino acid positions in the SP-D sequence. (B) Description of the designed peptide linkers and quantification of the FA present at the liposomal surface. (C) Tryptophan fluorescence of the tested peptides. A strong blue shift in the fluorescence emission maximum was observed for SP-DS3. (D) Molecular dynamics simulation of the interaction of SP-DS3 with the PC/CH membrane. The tryptophan residue (yellow) in an apolar environment and the FA (orange) at the membrane surface. (E) Representative TEM images of liposomes. Scale bar (red) represents 200 nm in smaller magnification and 20 nm in higher magnification.

Culture Collection. Cells were maintained in Dulbecco's modified Eagle medium (DMEM) containing 4 mM L-glutamine, 4.5 g/L glucose, and 1.5 g/L sodium bicarbonate supplemented with 10% (v/v) of fetal bovine serum (FBS), 1% (v/v) penicillin/streptomycin solution, and 1% (v/v) nonessentials amino acids. The cells were maintained at 37 °C in a humidified atmosphere of 5% CO_2. Caco-2 cells were routinely subcultured over 7 days, and the culture medium was replaced every 2 days. Caco-2 cells were plated at 10^6 cells/well in six-well dishes for 10 days. Cells were stimulated by incubation with a mixture of proinflammatory cytokines (Cytomix; 40 ng/mL each of interferon-γ, interleukin-1β and tumor necrosis factor (TNFα) for 16 h.

Cell Viability Assay. Cells were seeded at a density of 10×10^3 cells per 100 μL per well on 96-well TCPS plates (TPP, Switzerland) the day before the experiments and then exposed to different liposome and drug concentrations. At determined time of exposure, cell viability was determined using a 3-(4,5-dimethylthiazol-2-yl)-5-(3-carboxymethoxyphenyl)-2-(4-sulfophenyl)-2H-tetrazolium (MTS) assay. A ready-for-use CellTiter 96 Aqueous One solution of MTS (Promega, Madison, WI) was used according to the protocol suggested by the manufacturer. The culture medium was refreshed, and 20 μL of CellTiter 96 Aqueous One solution was added to each well. After 4 h of incubation at 37 °C, the absorbance at 490 nm was measured using a microplate reader (Spectramax 340PC).

Cytometer Analysis. The determination of fluorescence intensity was assessed by flow cytometer analysis, using FACScalibur from BD Biosciences. Briefly, cells were incubated for 1 h with 100 μg/mL liposomes in complete medium at 37 °C. As a negative control, macrophages were incubated just with complete medium. After incubation, cells were washed twice with PBS (pH 7.4) and then resuspended in PBS for fluorescence-activated cell sorting (FACS) analysis. The internalization was determined as the geometrical mean fluorescence intensity of liposomes corrected for the background staining of cells incubated with no nanoparticles (negative control) and normalized by the internalization level of each formulation.

Confocal Laser Scanning Microscopy (CLSM). Multilamellar vesicles of liposomes incorporating SP-DS3 were used as a model to perform CLSM experiments with a Leica TCS SPE confocal microscope (Leica Microsystems GmbH, Mannheim, Germany). Laser light wavelengths of 488 nm were used for the excitation of Oregon Green 488. The emitted light was detected in the range of 500−556 nm. Every optical field, laser intensity, photomultiplier gain and offset was individually adjusted to optimize the signal/noise ratio. Confocal stacks were acquired with an ACS APO 63.0× 1.30 oil-immersion objective lens while applying a Z-step of 6.01 μm. For liposomal internalization studies, Caco-2 cells were seeded at a density of 5×10^5 cells per 500 μL per well on 22 mm coverslips inserted into the wells of 24-well tissue culture polystyrene (TCPS) plates (TPP, Switzerland). After 10 days of adhesion, with the medium refreshed every 2 days, the medium was removed, and cells were washed twice with PBS. The cells were incubated with FR-targeted liposomes and nontargeted control liposomes, labeled with FITC at a phospholipid concentration of 100 μg/mL and diluted in Hank's balanced salt solution (HBSS) medium. After 1.5 h of exposure, the medium was removed, and cells were washed three times with acid and basic PBS at 4 °C to remove receptor-bound free folate and not internalized liposomes. The cells were then fixed with 4% paraformaldehyde for 30 min. The cells were further washed three times with PBS. After drying, the coverslips were put on slides coated with 2 μL of Vectashield mounting medium (VECTOR) and sealed. Slides were examined using an inverted Zeiss confocal laser scanning microscope (CLSM, Olympus Fluoview FV1000). Volume rendering and 3D models were created with the software Imaris7.0 (Bitplane, Zurich, Switzerland).

RNA Isolation, cDNA Synthesis and Quantitative Reverse Transcription Polymerase Chain Reaction (RT-PCR). Total RNA was extracted using the SV Total RNA Isolation System (Promega) according to the manufacturer's instructions and quantified with a NanoDrop ND-1000 spectrophotometer (Nanodrop Technologies, Wilmington, DE). Reverse transcription (RT) was performed using the iScript cDNA synthesis kit (BioRad) with a unique blended oligo(dT) and random hexamer primers, according to the manufacturer's protocols. Quantification of gene expression was performed with a CFX96 Real Time PCR Detection System from BioRad using reagents and protocols from the TaqMan Gene Expression Assay Protocol (Applied Biosystems). Each sample was normalized against the expression of mitochondrially encoded ATP synthase (MT-ATP6) as a stable internal control. The assay IDs of the TaqMan Gene Expression Assays were Hs02596862_g1 (MT-ATP6), Hs00153133_m1 (COX-2), HS00174103_m1 (IL-8), and Hs01042796_m1 (MMP7).

Statistical Analysis. Statistical analyses were performed with GraphPad Prism software (version 5.0). Unless otherwise stated,

DOI: 10.1021/acs.biomac.5b00823
Biomacromolecules XXXX, XXX, XXX−XXX

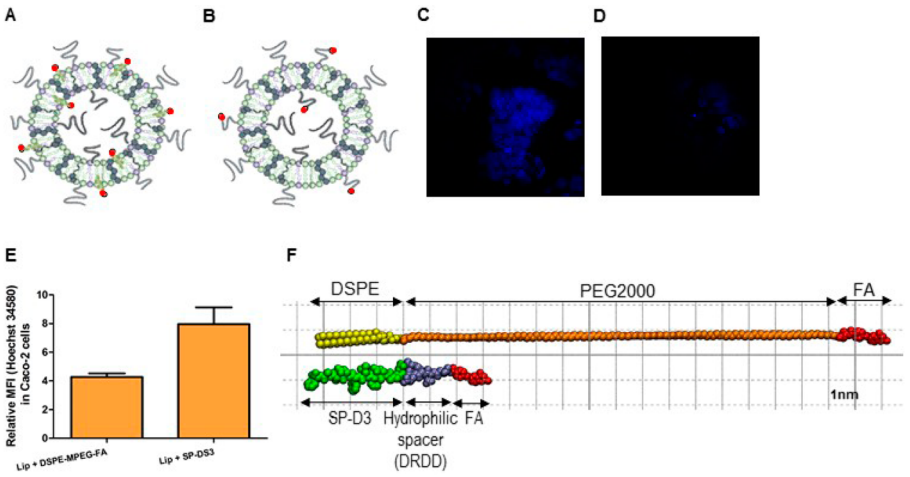

Figure 2. Liposomes with FA conjugated to SP-DS3 peptide are more efficiently disrupted compared to DSPE-PEG-FA. (A) Schematic representation of liposomes incorporating SP-DS3 peptide and (B) DSPE-PEG-FA. Representative pictures of the Caco-2 cells (FR+) after 1 h of incubation with fluorescent liposomal formulations (Hoechst 34580, blue staining) (C) with SP-DS3 and (D) DSPE-PEG-FA. (E) Efficient membrane disruption of liposomes incorporating SP-DS3 peptide, comparing with DSPE-PEG-FA, by Caco-2 cells. Graphs represent the relative mean fluorescence intensity (MFI) determined by flow cytometry analysis of Hoechst 34580 in Caco-2 cells with internalized liposomes after 1 h of incubation at 37 °C. Values are the mean + SD of 2 experiments. (F) Structures of DSPE-PEG-FA and SP-DS3.

differences were tested for statistical significance by a one-way ANOVA.

RESULTS AND DISCUSSION

Interaction of Peptide with Liposomes. We started by analyzing the interaction of three different peptide sequences (corresponding to amino acids 235−248 of SP-D; Figure 1A) with a liposomal formulation composed of DOPE/CH/DSPE-MPEG. At the N-terminus of the peptide, a hydrophilic bifunctional peptide spacer (DRDD) previously described in the literature, was added to improve the aqueous solubility of the final FA conjugate under physiological conditions.[17,18] The quantification of FA at the liposomal surface (Figure 1B) demonstrated the utility using of this hydrophilic spacer as liposomes with a peptide linker lacking the spacer DRDD (SP-D3) did not show quantifiable FA at the surface in contrast to liposomes with peptide linkers SP-DS1 and SP-DS3. Furthermore, SP-DS2 presence led to a reduced FA concentration at the surface and thus was excluded in subsequent studies. Tryptophan fluorescence and a photoactivatable phosphatidylcholine analogue were used to discriminate between deep insertion of the peptide in the bilayer and poor adsorption at the membrane surface. A tryptophan residue was included at position 5 from the C-terminus of the peptide sequence. A blue shift in the wavelength of maximum fluorescence emission is known to occur when tryptophan is transferred from a polar medium to a less polar environment. The results demonstrated that both peptide linkers penetrate into the liposomes; however, a pronounced blue shift was observed in the liposomal formulation using SP-DS3 (330 nm vs 342 nm for SP-DS1), suggesting that this peptide penetrates deeper into the non polar hydrocarbon region of the bilayer than does SP-DS1 (Figure 1C). A deep insertion of SP-DS3 prevents their dissociation from the liposome after intravenous injection. Therefore, this peptide was selected for further the studies.

To confirm the deep insertion of SP-DS3 in the bilayer, we used the photoactivatable phosphatidylcholine analogue [^{125}I]TID PC/16, which has been used to identify and characterize regions within membrane proteins that interact with lipids.[19] [^{125}I]TID PC/16 positions itself in the phospholipid milieu and, upon photolysis, reacts with the peptide if present in the vicinity.[20,21] During the reaction between the photoactivatable group and the peptide, the aryl group is transferred to the peptide and quantified via ^{125}I, demonstrating that SP-DS3 was incorporated in the phospholipid milieu. To further assess the behavior of SP-DS3 in the lipid bilayer, a molecular modeling study was performed using GROMACS software. The resultant model indicated that FA is located at the membrane surface, whereas SP-DS3 is deeply inserted into the lipid bilayer with the tryptophan residue in contact with the hydrocarbon region (Figure 1D). This model is consistent with the experimental results described above. CLSM analysis revealed the homogeneous distribution of SP-DS3 (with Oregon Green 488 dye covalently bound at the C-terminus) in contact with hydrophilic regions both on the liposomal surface of multilamellar vesicles (MLV) and in the aqueous core (data not shown). Using STEM (data not shown) and TEM (Figure 1E) imaging, we showed that nanocapsules of liposomes integrating SP-DS3 have a spherical form with a uniform diameter of approximately 120 nm. This size distribution was confirmed by dynamic light scattering (DLS) measurements (Table S1). Both liposomal formulations exhibited a narrow size distribution (polydispersity index <0.1), indicating that all liposome preparations had similar physicochemical characteristics. After 16 weeks of storage in PBS (pH 7.4) at 4 °C, the particle sizes of either formulations remained unaltered, suggesting a high stability of these liposomes in terms of size distribution. Furthermore, ζ-potential values remained unchanged (close to zero) during this time. To evaluate the cytotoxicity of the liposomal formulations, an important parameter for biological applications, cell viability, was assessed by several assays using immortalized cell lines. Liposomal formulations did not induce toxicity over a wide range of concentrations (up to 750 μg/mL and 72 h; Figure S3). Furthermore, liposomal formulations did not induce hemolysis in rat blood (Figure S4).

DOI: 10.1021/acs.biomac.5b00823
Biomacromolecules XXXX, XXX, XXX−XXX

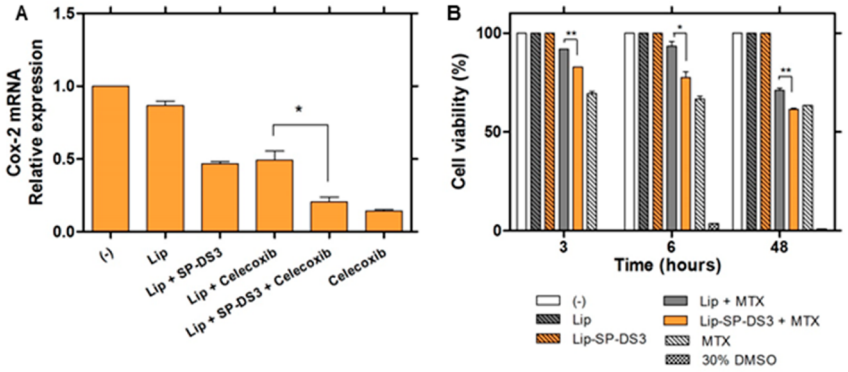

Figure 3. Liposomes integrating SP-DS3 are an efficient drug delivery system to FR-expressing cells. (A) The effects of 250 μg/mL of liposomal formulations with and without 65 μM celecoxib on COX-2 mRNA expression in Caco-2 cells (3 h of contact with liposomes +21 h of medium without liposomes). Values are the mean + SD of 2 experiments. (B) Caco-2 cell viability after 3, 6, and 48 h of contact with 10 μg/mL liposomal formulations encapsulating 1.27 μM methotrexate compared with untreated cells (negative control) and 30% DMSO-treated cells (positive control) as determined by the MTS assay at 48 h. Values are the mean + SD of 2 experiments. Significant differences were detected as shown by an asterisk ($P < 0.05$) and two asterisks ($P < 0.005$).

To evaluate the efficiency of FA targeting in liposomes integrating SP-DS3, we used a human colorectal carcinoma derived cell line (Caco-2) overexpressing FRα.[22,23] Caco-2 cells have also been used not only as an in vitro cancer model but also as a model of chronic inflammation.[24] The images obtained by CLSM showed that FR-targeting liposomes labeled with FITC are well internalized by FR-expressing Caco-2 cells in comparison with nontargeted control liposomes (Figure S5). In our recent study,[25] we measured the uptake of these FR-targeting liposomes in the monocytic cell line THP-1 with and without overexpression of human FRβ. Liposomes with FA were highly internalized by THP-1 cells retrovirally transformed with FRβ in comparison with the wild-type THP-1 cells, which weakly express FRβ, that showed minimal uptake.[25] Furthermore, the in vivo uptake specificity of these new liposomes in a pathological context of rheumatoid arthritis, was also measured. In comparison to liposomes without FA, SP-DS3 liposomes strongly accumulated in the joints of arthritic mice.[25] Furthermore, *in vivo* evaluation of the clinical benefit of liposomal formulations encapsulating the anti-inflammatory drug MTX, indicated that SP-DS3 liposomes loaded with MTX improved prophylactic efficacy and thus the mice did not show any clinical signs of the disease.[25]

Evaluation of the FA-Tailed Peptide Efficiency. The efficiency of liposomal membrane disruption was compared between the optimized liposomal formulation containing SP-DS3 peptide (Figure 2A) or DSPE-PEG-FA (Figure 2B), a commonly used FA conjugate.[26] In the present study, encapsulated Hoechst 34580 was used to evaluate the efficiency of liposomal membrane disruption, through detection of an eventual increase in blue fluorescence derived from to the specific binding of this dye to DNA. The results clearly indicate that liposomes with FA conjugated to SP-DS3 peptide are more efficiently disrupted in Caco-2 cells, and consequently may quickly deliver the vectorized compounds (Figures 2C,D and S6). Approximately 2-fold more Hoechst-associated fluorescence was detected by flow cytometer analysis with targeted liposomes incorporating SP-DS3, relatively to those prepared with DSPE-MPEG (Figure 2E). We propose that the mechanism of liposomal membrane disruption is more efficient due to the smaller size of the hydrophilic bifunctional peptide spacer (DRDD), as compared to PEG (Figure 2F). This implies that the close contact between liposome and cell can lead to major liposomal membrane deformation in the process of receptor binding and internalization, and consequently faster and more effective disruption.

Evaluation of Liposomes Incorporating FA-Tailed Peptide as a Drug Delivery System. We further tested the capacity of SP-DS3 liposomes to encapsulate and specifically deliver drugs into targeted cells. Liposomes loaded with one of two hydrophobic anti-inflammatory drugs, celecoxib and CORM-2, or a hydrophilic antiarthritic and antineoplastic FA analogue, MTX, were produced.[27,28] Physicochemical characterization was performed, and the respective data, similar to that obtained for unloaded liposomes (Table S1), indicate that drugs are encapsulated inside the liposomes. The concentration of encapsulated drug was determined for each liposomal formulation, and the biological effect was compared with that of the same concentration of free drug. Celecoxib is a selective inhibitor of cyclooxygenase-2 (COX-2) and exerts its effects by inhibiting the synthesis of prostaglandins involved in pain, fever, and inflammation.[29,30] Previous reports show that celecoxib strongly decreases protein expression of COX-2, which is directly proportional to a decrease of mRNA levels.[31−33] Since (q) PCR is a very sensitive technique, it was considered the best option to monitor this highly regulated pathway. We observed that celecoxib-loaded liposomes decreased the expression of COX-2 (Figure 3A), which is consistent with the fluorescence data showing that these liposomes can be internalized to some extent by Caco-2 cells. This reduction was much more pronounced in liposomes integrating SP-DS3, which showed similar levels to those obtained with celecoxib alone, indicating the effective release of the cargo from the targeted liposomes in vitro.

Similar results were obtained with SP-DS3 liposomes encapsulating CORM-2[34] assessed in Caco-2 cells stimulated with pro-inflammatory cytokines (Cytomix); mRNA levels of interleukin-8 (IL-8) and metalloproteinase-7 (MMP-7), which are crucial for cancer cell proliferation and invasion, were quantified.[24] A previous publication showed that CORM-2 simultaneously decreases both protein and mRNA levels of IL-8 and MMP-7.[24] Both mRNAs were strongly diminished compared with those from cells incubated with liposomes or CORM-2 alone (Figure S7). Of note was the effect of unloaded SP-DS3 liposomes in the expression of these inflammatory mediators as well as of COX-2. Indeed, the presence of FA,

DOI: 10.1021/acs.biomac.5b00823
Biomacromolecules XXXX, XXX, XXX−XXX

vitamin B9, is associated with an attenuation of inflammation and reduction in pro-inflammatory cytokine levels.[35] SP-DS3 liposomes were also tested for the efficient delivery of MTX. Liposomes encapsulating MTX significantly reduced the viability of Caco-2 cells (Figure 3B), whereas empty liposomes had no effect. This cytotoxic effect was enhanced in cells contacting SP-DS3 liposomes, suggesting preferential internalization of these targeted liposomes. Collectively, these data demonstrate that our delivery system is efficient in the encapsulation and specific delivery of both hydrophobic and hydrophilic drugs.

CONCLUSION

In conclusion, we have successfully developed novel FR-targeted liposomes by incorporating a bifunctional SP-DS3 peptide consisting of the neck domain present in surfactant proteins, which serves as both a linker and an anchor of the FA to the liposomal membrane. This peptide, linked to a specific hydrophilic peptide spacer, was shown to insert deeply into the lipid bilayer without affecting the integrity of the liposomes. Furthermore, our delivery system was proved to be more efficient than classic systems where the FA is linked to liposomes by PEG. The combination of all complementary characteristics of these tailored liposomes, including their small size, lack of cytotoxicity and their specific targeting of FR-expressing cells, supports their use as specific therapeutic nanodelivery systems as demonstrated here by the biological effect of several drugs. The use of liposomes equipped with the novel bifunctional SP-DS3 peptide linker reported here for FA-mediated delivery opens new opportunities for the treatment of human diseases, including chronic inflammatory diseases and cancer.

ASSOCIATED CONTENT

Supporting Information

Data of SP-DS3 characterization by analytical high-performance liquid chromatography and mass spectrometry are provided as Supporting Information. Furthermore, physicochemical characterization, cell viability, hemolytic properties and specificity of liposomal formulations, as well the biological effect of liposomes encorporating CORM-2 are included. The Supporting Information is available free of charge on the ACS Publications website at DOI: 10.1021/acs.biomac.5b00823.

(PDF)

AUTHOR INFORMATION

Corresponding Author

*Phone: 00351253604409. Fax: 00351253604429. E-mail: artur@deb.uminho.pt.

Notes

The authors declare the following competing financial interest(s): A.C.P., A.P., E.N. and A.C.G. filed for a patent to use the SP-DS3 peptide in FA-targeted liposomes for specific drug delivery.

ACKNOWLEDGMENTS

Eugénia Nogueira (SFRH/BD/81269/2011) and Ana Loureiro (SFRH/BD/81479/2011) hold scholarships from Fundação para a Ciência e a Tecnologia (FCT). Gonçalo J. L. Bernardes is a Royal Society University Research Fellow at the Department of Chemistry, University of Cambridge and an Investigador FCT at the Instituto de Medicina Molecular, Faculdade de Medicina da Universidade de Lisboa. This study was funded by the European Union Seventh Framework Programme (FP7/2007-2013) under grant agreement NMP4-LA-2009-228827 NANOFOL. The authors thank the FCT Strategic Project of UID/BIO/04469/2013 unit, the project RECI/BBB-EBI/0179/2012 (FCOMP-01-0124-FEDER-027462) and the Project "BioHealth - Biotechnology and Bioengineering approaches to improve health quality", Ref. NORTE-07-0124-FEDER-000027, co-funded by the Programa Operacional Regional do Norte (ON.2 – O Novo Norte), QREN, FEDER. This work was also supported by FCT I.P. through the strategic funding UID/BIA/04050/2013. We also thank Noëmy Gueriba for her technical assistance in various experiments.

REFERENCES

(1) Sant, V. P.; Nagarsenker, M. S. *AAPS PharmSciTech* **2011**, *12* (4), 1056–63.
(2) Low, P. S.; Henne, W. A.; Doorneweerd, D. D. *Acc. Chem. Res.* **2008**, *41* (1), 120–9.
(3) Hilgenbrink, A. R.; Low, P. S. *J. Pharm. Sci.* **2005**, *94* (10), 2135–2146.
(4) Low, P. S.; Kularatne, S. A. *Curr. Opin. Chem. Biol.* **2009**, *13* (3), 256–262.
(5) Gabizon, A.; Shmeeda, H.; Horowitz, A. T.; Zalipsky, S. *Adv. Drug Delivery Rev.* **2004**, *56* (8), 1177–1192.
(6) Liu, Y.; Xu, S.; Teng, L.; Yung, B.; Zhu, J.; Ding, H.; Lee, R. J. *Anticancer Res.* **2011**, *31* (5), 1521–1525.
(7) Xiong, S.; Yu, B.; Wu, J.; Li, H.; Lee, R. J. *Biomed. Pharmacother.* **2011**, *65* (1), 2–8.
(8) Seo, H. J.; Kim, J.-C. *Bioconjugate Chem.* **2014**, *25* (3), 533–542.
(9) Xiang, G.; Wu, J.; Lu, Y.; Liu, Z.; Lee, R. J. *Int. J. Pharm.* **2008**, *356* (1–2), 29–36.
(10) Zhang, P.; McAlinden, A.; Li, S.; Schumacher, T.; Wang, H.; Hu, S.; Sandell, L.; Crouch, E. *J. Biol. Chem.* **2001**, *276* (23), 19862–19870.
(11) Kingma, P. S.; Whitsett, J. A. *Curr. Opin. Pharmacol.* **2006**, *6* (3), 277–283.
(12) Kishore, U.; Greenhough, T. J.; Waters, P.; Shrive, A. K.; Ghai, R.; Kamran, M. F.; Bernal, A. L.; Reid, K. B. M.; Madan, T.; Chakraborty, T. *Mol. Immunol.* **2006**, *43* (9), 1293–1315.
(13) Mangialavori, I.; Giraldo, A. M. V.; Buslje, C. M.; Gomes, M. F.; Caride, A. J.; Rossi, J. P. F. C. *J. Biol. Chem.* **2009**, *284* (8), 4823–4828.
(14) Hess, B.; Kutzner, C.; van der Spoel, D.; Lindahl, E. *J. Chem. Theory Comput.* **2008**, *4* (3), 435–447.
(15) Hess, B.; Bekker, H.; Berendsen, H. J. C.; Fraaije, J. G. E. M. *J. Comput. Chem.* **1997**, *18* (12), 1463–1472.
(16) Berendsen, H. J. C.; Postma, J. P. M.; van Gunsteren, W. F.; DiNola, A.; Haak, J. R. *J. Chem. Phys.* **1984**, *81* (8), 3684.
(17) Vlahov, I. R.; Wang, Y.; Kleindl, P. J.; Leamon, C. P. *Bioorg. Med. Chem. Lett.* **2008**, *18* (16), 4558–4561.
(18) Leamon, C. P.; Reddy, J. A.; Vlahov, I. R.; Westrick, E.; Parker, N.; Nicoson, J. S.; Vetzel, M. *Int. J. Cancer* **2007**, *121* (7), 1585–1592.
(19) Durrer, P.; Galli, C.; Hoenke, S.; Corti, C.; Glück, R.; Vorherr, T.; Brunner, J. *J. Biol. Chem.* **1996**, *271* (23), 13417–13421.
(20) Giraldo, A. M. V.; Castello, P. R.; Flecha, F. L. G.; Moeller, J. V.; Delfino, J. M.; Rossi, J. P. F. C. *FEBS Lett.* **2006**, *580* (2), 607–612.
(21) Mangialavori, I. C.; Caride, A. J.; Rossi, R. C.; Rossi, J. P. F. C.; Strehler, E. E. *Curr. Chem. Biol.* **2011**, *5* (2), 118–129.
(22) Weitman, S. D.; Lark, R. H.; Coney, L. R.; Fort, D. W.; Frasca, V.; Zurawski, V. R., Jr.; Kamen, B. A. *Cancer Res.* **1992**, *52* (12), 3396–401.
(23) Roger, E.; Kalscheuer, S.; Kirtane, A.; Guru, B. R.; Grill, A. E.; Whittum-Hudson, J.; Panyam, J. *Mol. Pharmaceutics* **2012**, *9* (7), 2103–10.
(24) Megías, J.; Busserolles, J.; Alcaraz, M. J. *Br. J. Pharmacol.* **2007**, *150* (8), 977–986.

DOI: 10.1021/acs.biomac.5b00823
Biomacromolecules XXXX, XXX, XXX–XXX

(25) Nogueira, E.; Lager, F.; Le Roux, D.; Nogueira, P.; Freitas, J.; Charvet, C.; Renault, G.; Loureiro, A.; Almeida, C. R.; Ohradanova-Repic, A.; Machacek, C.; Bernardes, G. J. L.; Moreira, A.; Stockinger, H.; Burnet, M.; Carmo, A. M.; Gomes, A. C.; Preto, A.; Bismuth, G.; Cavaco-Paulo, A. *J. Biomed. Nanotechnol.* **2015**, *11*, 2243−2252.
(26) Gabizon, A.; Tzemach, D.; Gorin, J.; Mak, L.; Amitay, Y.; Shmeeda, H.; Zalipsky, S. *Cancer Chemother. Pharmacol.* **2010**, *66* (1), 43−52.
(27) Chan, E. S. L.; Cronstein, B. N. *Nat. Rev. Rheumatol.* **2010**, *6* (3), 175−178.
(28) Genestier, L.; Paillot, R.; Quemeneur, L.; Izeradjene, K.; Revillard, J.-P. *Immunopharmacology* **2000**, *47* (2−3), 247−257.
(29) Kısmet, K.; Akay, M. T.; Abbasoğlu, O.; Ercan, A. *Cancer Detect. Prev.* **2004**, *28* (2), 127−142.
(30) Cui, W.; Yu, C.-H.; Hu, K.-Q. *Clin. Cancer Res.* **2005**, *11* (22), 8213−8221.
(31) Zhao, S.-p.; Deng, P.; Huang, H.-g.; Xu, Z.-m.; Dai, H.-y.; Hong, S.-c.; Yang, J.; Zhou, H.-n. *Clin. Chem.* **2005**, *51* (11), 2170−2173.
(32) Zhang, G. S.; Liu, D. S.; Dai, C. W.; Li, R. J. *Am. J. Hematol.* **2006**, *81* (4), 242−55.
(33) Dai, Z.-J.; Ma, X.-B.; Kang, H.-F.; Gao, J.; Min, W.-L.; Guan, H.-T.; Diao, Y.; Lu, W.-F.; Wang, X.-J. *Cancer Cell Int.* **2012**, *12* (1), 53.
(34) Romao, C. C.; Blattler, W. A.; Seixas, J. D.; Bernardes, G. J. L. *Chem. Soc. Rev.* **2012**, *41* (9), 3571−3583.
(35) Kolb, A. F.; Petrie, L. *Mol. Immunol.* **2013**, *54* (2), 164−172.

DOI: 10.1021/acs.biomac.5b00823
Biomacromolecules XXXX, XXX, XXX−XXX